



CERN-EP-2018-156
 LHCb-PAPER-2018-022
 June 20, 2018

Observation of the decay $\Lambda_b^0 \rightarrow \psi(2S)p\pi^-$

LHCb collaboration[†]

Abstract

The Cabibbo-suppressed decay $\Lambda_b^0 \rightarrow \psi(2S)p\pi^-$ is observed for the first time using a data sample collected by the LHCb experiment in proton-proton collisions corresponding to 1.0, 2.0 and 1.9 fb^{-1} of integrated luminosity at centre-of-mass energies of 7, 8 and 13 TeV, respectively. The $\psi(2S)$ mesons are reconstructed in the $\mu^+\mu^-$ final state. The branching fraction with respect to that of the $\Lambda_b^0 \rightarrow \psi(2S)pK^-$ decay mode is measured to be

$$\frac{\mathcal{B}(\Lambda_b^0 \rightarrow \psi(2S)p\pi^-)}{\mathcal{B}(\Lambda_b^0 \rightarrow \psi(2S)pK^-)} = (11.4 \pm 1.3 \pm 0.2)\%,$$

where the first uncertainty is statistical and the second is systematic. The $\psi(2S)p$ and $\psi(2S)\pi^-$ mass spectra are investigated and no evidence for exotic resonances is found.

Published in JHEP 1808 (2018) 131

© 2018 CERN for the benefit of the LHCb collaboration. CC-BY-4.0 licence.

[†]Authors are listed at the end of this paper.

1 Introduction

The Λ_b^0 baryon is the isospin-singlet ground state of a bound system of a beauty quark and two light quarks. The high production rate of b quarks at the Large Hadron Collider (LHC) [1–5], along with the excellent mass resolution and hadron-identification capabilities of the LHCb detector, give access to a variety of decay channels of the Λ_b^0 baryon, including multibody, rare, charmless and semileptonic decays [6–25]. The high signal yield of the $\Lambda_b^0 \rightarrow J/\psi p K^-$ decay [15] facilitated a precise measurement of the Λ_b^0 lifetime [26], while the relatively low energy released in the $\Lambda_b^0 \rightarrow \psi(2S)p K^-$ and $\Lambda_b^0 \rightarrow \chi_c p K^-$ decays allowed for precise measurements of the Λ_b^0 mass [16, 22]. A six-dimensional amplitude analysis of the $\Lambda_b^0 \rightarrow J/\psi p K^-$ decay resulted in the observation of the $P_c(4380)^+$ and $P_c(4450)^+$ pentaquark states decaying into the $J/\psi p$ final state [27]. Later, these states were confirmed using a model-independent technique [28]. Subsequently, an analysis of Cabibbo-suppressed $\Lambda_b^0 \rightarrow J/\psi p \pi^-$ decays found evidence for contributions from the $P_c(4380)^+$ and $P_c(4450)^+$ pentaquarks and from the $Z_c(4200)^-$ tetraquark [29].

The first observation of Λ_b^0 decays to the excited charmonium state $\psi(2S)$ was made in the $\Lambda_b^0 \rightarrow \psi(2S)\Lambda$ decay mode by the ATLAS collaboration [30]. Later, the decay $\Lambda_b^0 \rightarrow \psi(2S)p K^-$ was observed by the LHCb collaboration [16]. The Cabibbo-suppressed analogue of the latter decay, $\Lambda_b^0 \rightarrow \psi(2S)p \pi^-$, is of particular interest because of possible contributions from exotic states in both the $\psi(2S)p$ system, similar to the $P_c(4380)^+$ and $P_c(4450)^+$ pentaquark states, and in the $\psi(2S)\pi^-$ system, analogous to the charged charmonium-like state $Z_c(4430)^-$ studied in detail by the Belle and LHCb collaborations in $B \rightarrow \psi(2S)\pi^- K$ decays [31–35]. Depending on the nature of a proposed exotic state, its coupling with the $\psi(2S)$ meson can be larger than with the J/ψ meson. For example, the decay rate of the $X(3872)$ particle to the $\psi(2S)\gamma$ final state was found to exceed the corresponding decay rate to the $J/\psi\gamma$ final state [36, 37].

This paper reports the first observation of the decay $\Lambda_b^0 \rightarrow \psi(2S)p \pi^-$ using a data sample collected by the LHCb experiment in proton-proton collisions corresponding to 1.0, 2.0 and 1.9 fb^{-1} of integrated luminosity at centre-of-mass energies of 7, 8 and 13 TeV, respectively. A measurement is made of the $\Lambda_b^0 \rightarrow \psi(2S)p \pi^-$ branching fraction relative to that of the Cabibbo-favoured decay $\Lambda_b^0 \rightarrow \psi(2S)p K^-$,

$$R_{\pi/K} \equiv \frac{\mathcal{B}(\Lambda_b^0 \rightarrow \psi(2S)p \pi^-)}{\mathcal{B}(\Lambda_b^0 \rightarrow \psi(2S)p K^-)}, \quad (1)$$

where the $\psi(2S)$ mesons are reconstructed in the $\mu^+ \mu^-$ final state. Throughout this paper the inclusion of charge-conjugated processes is implied.

2 Detector and simulation

The LHCb detector [38, 39] is a single-arm forward spectrometer covering the pseudorapidity range $2 < \eta < 5$, designed for the study of particles containing b or c quarks. The detector includes a high-precision tracking system consisting of a silicon-strip vertex detector surrounding the pp interaction region, a large-area silicon-strip detector located upstream of a dipole magnet with a bending power of about 4 Tm, and three stations of silicon-strip detectors and straw drift tubes placed downstream of the magnet. The tracking system provides a measurement of the momentum

of charged particles with a relative uncertainty that varies from 0.5% at low momentum to 1.0% at $200\text{ GeV}/c$. The minimum distance of a track to a primary vertex (PV), the impact parameter (IP), is measured with a resolution of $(15 + 29/p_T)\mu\text{m}$, where p_T is the component of the momentum transverse to the beam, in GeV/c . Different types of charged hadrons are distinguished using information from two ring-imaging Cherenkov detectors (RICH). Photons, electrons and hadrons are identified by a calorimeter system consisting of scintillating-pad and preshower detectors, an electromagnetic calorimeter and a hadronic calorimeter. Muons are identified by a system composed of alternating layers of iron and multiwire proportional chambers.

The online event selection is performed by a trigger [40], which consists of a hardware stage, based on information from the calorimeter and muon systems, followed by a software stage, which applies a full event reconstruction. The hardware trigger selects muon candidates with high transverse momentum or dimuon candidates with high value of the product of the p_T of each muon. The subsequent software trigger is composed of two stages, the first of which performs a partial event reconstruction, while full event reconstruction is done at the second stage. In the software trigger, each pair of oppositely charged muons forming a good-quality two-track vertex is required to be significantly displaced from all PVs and the mass of the pair is required to exceed $2.7\text{ GeV}/c^2$.

The techniques used in this analysis are validated using simulated events. In the simulation, pp collisions are generated using PYTHIA [41] with a specific LHCb configuration [42]. Decays of hadronic particles are described by EVTGEN [43], in which final-state radiation is generated using PHOTOS [44]. The interaction of the generated particles with the detector, and its response, are implemented using the GEANT4 toolkit [45] as described in Ref. [46].

3 Event selection

The signal $\Lambda_b^0 \rightarrow \psi(2S)p\pi^-$ and the normalization $\Lambda_b^0 \rightarrow \psi(2S)pK^-$ decays are both reconstructed using the decay mode $\psi(2S) \rightarrow \mu^+\mu^-$. Similar selection criteria, based on those used in Ref. [16], are applied to both channels.

Muon, proton, pion and kaon candidates are identified using combined information from the RICH, calorimeter and muon detectors. They are required to have a transverse momentum larger than 550, 900, 500 and 200 MeV/c , respectively. To allow for an efficient particle identification, kaons and pions are required to have a momentum between 3.2 and 150 GeV/c , whilst protons must have a momentum between 10 and 150 GeV/c . To reduce the combinatorial background due to particles produced in the pp interaction, only tracks that are inconsistent with originating from a PV are used.

Pairs of oppositely charged muons consistent with originating from a common vertex are combined to form $\psi(2S) \rightarrow \mu^+\mu^-$ candidates. The mass of the dimuon candidate is required to be between 3.67 and $3.70\text{ GeV}/c^2$, where the asymmetric mass range around the known $\psi(2S)$ mass [47] is chosen to account for final-state radiation. The position of the reconstructed dimuon vertex is required to be inconsistent with that of any of the reconstructed PVs.

To form signal (normalization) Λ_b^0 candidates, the selected $\psi(2S)$ candidates are combined with a proton and a pion (kaon) of opposite charges. Each Λ_b^0 candidate is associated with the PV with respect to which it has the smallest χ_{IP}^2 , where χ_{IP}^2 is defined

as the difference in the vertex-fit χ^2 of a given PV reconstructed with and without the particle under consideration. To improve the Λ_b^0 mass resolution, a kinematic fit [48] is performed. This fit constrains the four charged final-state particles to form common vertex, the mass of the $\mu^+\mu^-$ combination to the known $\Psi(2S)$ mass and the Λ_b^0 candidate to originate from the associated PV. A good quality of this fit is required to further suppress combinatorial background. In addition, the measured decay time of the Λ_b^0 candidate, calculated with respect to the associated PV, is required to be between 0.2 and 2.0 mm/ c to suppress poorly reconstructed candidates and background from particles originating from the PV.

To suppress cross-feed from $B^0 \rightarrow \Psi(2S)K^+\pi^-$ decays with the positively charged kaon (negatively charged pion) misidentified as a proton (antiproton) for the signal (normalization) channel, a veto is applied on the Λ_b^0 candidate mass recalculated with a kaon (pion) mass hypothesis for the proton. Any candidate with a recalculated mass consistent with the nominal B^0 mass is rejected. A similar veto is applied to suppress cross-feed from $B_s^0 \rightarrow \Psi(2S)K^+K^-$ decays with the positively charged kaon misidentified as a proton, and additionally for the signal channel, the negatively charged kaon misidentified as a pion. Finally, to suppress cross-feed from the $\Lambda_b^0 \rightarrow \Psi(2S)\Lambda$ decay, followed by a $\Lambda \rightarrow p\pi^-$ decay, candidates with a $p\pi^-$ mass that is consistent with the nominal Λ mass [47] are rejected.

4 Signal yields and efficiencies

The mass distributions for the selected $\Lambda_b^0 \rightarrow \Psi(2S)p\pi^-$ and $\Lambda_b^0 \rightarrow \Psi(2S)pK^-$ candidates are shown in Fig. 1. The signal yields are determined using unbinned extended maximum-likelihood fits to these distributions. For each distribution the Λ_b^0 component is described by a modified Gaussian function with power-law tails on both sides [49, 50]. The tail parameters are fixed to values obtained from simulation, and the peak position and resolution of the Gaussian function are free to vary in the fit. The combinatorial background component is described by a monotonic second-order polynomial function with positive curvature. The resolution parameters obtained from the fits are found to be 5.23 ± 0.55 MeV/ c^2 for the $\Lambda_b^0 \rightarrow \Psi(2S)p\pi^-$ channel and 3.96 ± 0.13 MeV/ c^2 for the $\Lambda_b^0 \rightarrow \Psi(2S)pK^-$ channel, which are in good agreement with expectations from simulation. The signal yields are determined to be 121 ± 13 and 806 ± 29 for the $\Lambda_b^0 \rightarrow \Psi(2S)p\pi^-$ and $\Lambda_b^0 \rightarrow \Psi(2S)pK^-$ decay modes, respectively.

The resonance structure of the $\Lambda_b^0 \rightarrow \Psi(2S)p\pi^-$ decay is investigated using the *sPlot* technique [51] for background subtraction, with the reconstructed $\Psi(2S)p\pi^-$ mass as the discriminating variable. The background-subtracted mass distributions of $\Psi(2S)p$, $\Psi(2S)\pi^-$ and $p\pi^-$ combinations are shown in Fig. 2, along with those obtained from simulated decays generated according to a phase-space model. The $\Psi(2S)p$ and $\Psi(2S)\pi^-$ mass distributions show no evidence for contributions from exotic states. The mass distribution of the $p\pi^-$ combination differs from the phase-space model, indicating possible contributions from excited N^0 and Δ^0 states. Further studies with a larger data sample will provide a deeper insight into the underlying structure of the $\Lambda_b^0 \rightarrow \Psi(2S)p\pi^-$ decay.

The ratio of branching fractions $R_{\pi/K}$, defined in Eq. (1), is measured as

$$R_{\pi/K} = \frac{N_{\Lambda_b^0 \rightarrow \Psi(2S)p\pi^-}}{N_{\Lambda_b^0 \rightarrow \Psi(2S)pK^-}} \frac{\varepsilon_{\Lambda_b^0 \rightarrow \Psi(2S)pK^-}}{\varepsilon_{\Lambda_b^0 \rightarrow \Psi(2S)p\pi^-}}, \quad (2)$$

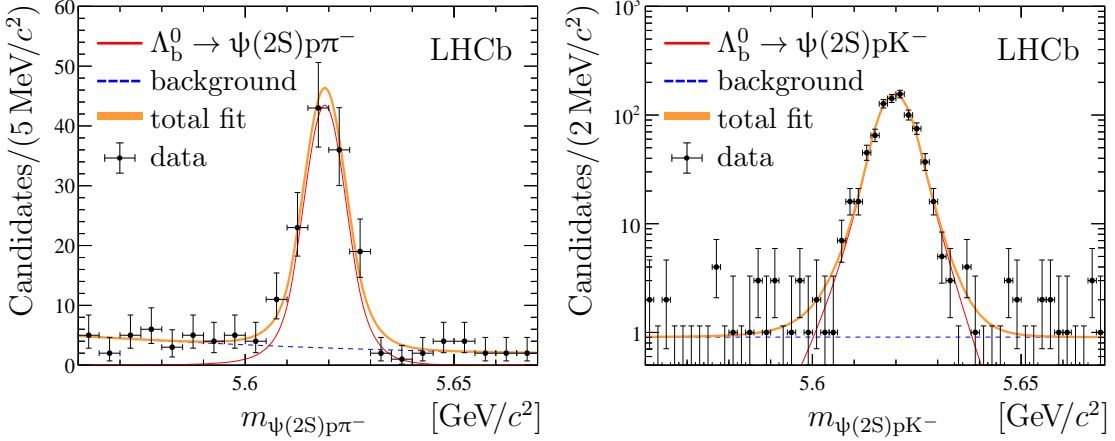


Figure 1: Mass distributions of the (left) $\Lambda_b^0 \rightarrow \psi(2S)p\pi^-$ and (right) $\Lambda_b^0 \rightarrow \psi(2S)pK^-$ candidates.

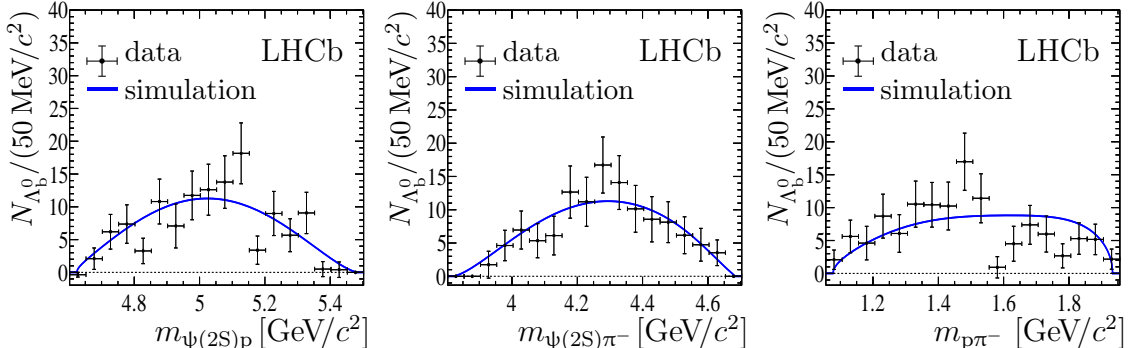


Figure 2: Background-subtracted mass distributions of the (left) $\psi(2S)p$, (centre) $\psi(2S)\pi^-$ and (right) $p\pi^+$ combinations in the $\Lambda_b^0 \rightarrow \psi(2S)p\pi^-$ decay compared with distributions obtained from a phase-space simulation.

where N represents the measured yield and ε denotes the efficiency of the corresponding decay. The efficiency is defined as the product of the geometric acceptance and the detection, reconstruction, selection and trigger efficiencies. The hadron-identification efficiencies as functions of kinematics and the event multiplicity are determined from data using the following calibration samples of low-background decays: $D^{*+} \rightarrow D^0(\rightarrow K^-\pi^+)\pi^+$, $K_s^0 \rightarrow \pi^+\pi^-$ and $D_s^+ \rightarrow \phi(\rightarrow K^+K^-)\pi^+$ for kaons and pions; and $\Lambda \rightarrow p\pi^-$ and $\Lambda_c^+ \rightarrow pK^+\pi^-$ for protons [52,53]. The remaining efficiencies are determined using simulation. The p_T and rapidity spectra and the lifetime of the Λ_b^0 baryons in simulated samples are adjusted to match those observed in a high-yield low-background sample of reconstructed $\Lambda_b^0 \rightarrow J/\psi pK^-$ decays. The simulated samples are produced according to a phase-space decay model. The simulated $\Lambda_b^0 \rightarrow \psi(2S)pK^-$ decays are corrected to reproduce the pK^- mass and $\cos\theta_{pK^-}$ distributions observed in data, where θ_{pK^-} is the helicity angle of the pK^- system, defined as the angle between the momentum vectors of the kaon and Λ_b^0 baryon in the pK^- rest frame. To account for imperfections in the simulation of charged tracks, corrections obtained using data-driven techniques are also applied [54].

The efficiencies are determined separately for each data-taking period and are combined according to the corresponding luminosity [55] for each period and the known production cross-section of $b\bar{b}$ pairs in the LHCb acceptance [1–5]. The ratio of the total efficiency of

the normalization channel to that of the signal channel is determined to be

$$\frac{\epsilon_{\Lambda_b^0 \rightarrow \psi(2S)pK^-}}{\epsilon_{\Lambda_b^0 \rightarrow \psi(2S)p\pi^-}} = 0.761 \pm 0.004, \quad (3)$$

where only the uncertainty that arises from the sizes of the simulated samples is given. Additional sources of uncertainty are discussed in the following section. The kaon identification efficiency, entering into $\epsilon_{\Lambda_b^0 \rightarrow \psi(2S)pK^-}$, is the main factor causing non-equality of the total efficiencies for the signal and normalization channels.

5 Systematic uncertainties

Since the signal and normalization decay channels have similar kinematics and topologies, most systematic uncertainties cancel in the ratio $R_{\pi/K}$, *e.g.* those related to muon identification. The remaining contributions to the systematic uncertainty are listed in Table 1 and discussed below.

To estimate the systematic uncertainty related to the fit model, pseudoexperiments are sampled from the baseline fit models with all parameters fixed from those obtained from the fits to the data. For each pseudoexperiment fits are performed with a number of alternative models for the signal and background components and the ratio $R_{\pi/K}$ is computed. A generalized Student's t-distribution [56] and an Apollonios function [57] are used as alternative models for the signal component, while polynomial functions of the second and the third order with various constraints for monotonicity and convexity are used as alternative backgrounds. The maximum relative bias found for $R_{\pi/K}$ is 0.7%, which is assigned as a relative systematic uncertainty.

The uncertainty related to the imperfect knowledge of the Λ_b^0 decay model used for the simulation of the $\Lambda_b^0 \rightarrow \psi(2S)pK^-$ decays is estimated by varying the correction factors obtained from kinematic distributions observed in data. Changing these correction factors within their statistical uncertainties causes a negligible variation of the efficiency $\epsilon_{\Lambda_b^0 \rightarrow \psi(2S)pK^-}$. For the $\Lambda_b^0 \rightarrow \psi(2S)p\pi^-$ signal decays the observed two-body mass distributions are in agreement with the phase-space model used in the simulation. The corresponding uncertainty due to the unknown decay kinematics of the $\Lambda_b^0 \rightarrow \psi(2S)p\pi^-$ signal decays is small and therefore neglected.

An additional uncertainty arises from the differences between data and simulation, in particular those affecting the efficiency for the reconstruction of charged-particle tracks. The small difference in the track-finding efficiency between data and simulation is corrected using a data-driven technique [54]. The uncertainties in these correction factors together with the uncertainties in the hadron-identification efficiencies, related to the finite size of the calibration samples [52, 53], are propagated to the ratio of total efficiencies by means of pseudoexperiments. This results in a systematic uncertainty of 0.2% associated with the track reconstruction and hadron identification.

The systematic uncertainty on the efficiency of the trigger has been previously studied using high-yield $B^+ \rightarrow J/\psi K^+$ and $B^+ \rightarrow \psi(2S)K^+$ decays by comparing ratios of trigger efficiencies in data and simulation [58]. Based on these comparisons a relative uncertainty of 1.1% is assigned.

Another source of uncertainty is the potential disagreement between data and simulation in the estimation of efficiencies, due to effects not considered above. This is

Table 1: Relative systematic uncertainties for the ratio of branching fractions. The total uncertainty is the quadratic sum of the individual contributions.

Source	Uncertainty [%]
Fit model	0.7
Track reconstruction and hadron identification	0.2
Trigger	1.1
Selection criteria	1.0
Size of the simulation samples	0.5
Total	1.7

studied using a high-yield low-background sample of $\Lambda_b^0 \rightarrow J/\psi p K^-$ decays, by varying the selection criteria in ranges that lead to as much as $\pm 20\%$ differences in the measured signal yields. The resulting variations in the efficiency-corrected yields do not exceed 1% for all inspected selection criteria. The value of 1% is taken as a corresponding systematic uncertainty.

Finally, the 0.5% relative uncertainty in the ratio of efficiencies from Eq. (3) is assigned as a systematic uncertainty due to the finite size of the simulated samples.

6 Results and summary

The Cabibbo-suppressed decay $\Lambda_b^0 \rightarrow \psi(2S)p\pi^-$ is observed using a data sample collected by the LHCb experiment in proton-proton collisions corresponding to 1.0, 2.0 and 1.9 fb^{-1} of integrated luminosity at centre-of-mass energies of 7, 8 and 13 TeV, respectively. The observed yield of $\Lambda_b^0 \rightarrow \psi(2S)p\pi^-$ decays is 121 ± 13 . Using the $\Lambda_b^0 \rightarrow \psi(2S)pK^-$ decay as a normalization channel, the ratio of the branching fractions is measured to be

$$R_{\pi/K} = \frac{\mathcal{B}(\Lambda_b^0 \rightarrow \psi(2S)p\pi^-)}{\mathcal{B}(\Lambda_b^0 \rightarrow \psi(2S)pK^-)} = (11.4 \pm 1.3 \pm 0.2)\%,$$

where the first uncertainty is statistical and the second is systematic. Neglecting the resonance structures in the $\Lambda_b^0 \rightarrow \psi(2S)p\pi^-$ and $\Lambda_b^0 \rightarrow \psi(2S)pK^-$ decays, the calculated value for the ratio $R_{\pi/K}$ is

$$R_{\pi/K}^{\text{th}} \approx \frac{\Phi_3(\Lambda_b^0 \rightarrow \psi(2S)p\pi^-)}{\Phi_3(\Lambda_b^0 \rightarrow \psi(2S)pK^-)} \times \tan^2 \theta_C \simeq 11\%,$$

where Φ_3 denotes the full three-body phase-space and θ_C is the Cabibbo angle [59]. The measured value is in a good agreement with this estimate.

The branching fraction $\mathcal{B}(\Lambda_b^0 \rightarrow \psi(2S)p\pi^-)$ is calculated using the value of $\mathcal{B}(\Lambda_b^0 \rightarrow \psi(2S)pK^-) = (6.29 \pm 0.23 \pm 0.14^{+1.14}_{-0.90}) \times 10^{-5}$ [16] as

$$\mathcal{B}(\Lambda_b^0 \rightarrow \psi(2S)p\pi^-) = (7.17 \pm 0.82 \pm 0.33^{+1.30}_{-1.03}) \times 10^{-6},$$

where the first uncertainty is statistical, the second systematic (including the statistical and systematic uncertainties from $\mathcal{B}(\Lambda_b^0 \rightarrow \psi(2S)pK^-)$) and the third arises from

the uncertainties in the branching fractions of the $\Lambda_b^0 \rightarrow J/\psi p K^-$, $\psi(2S) \rightarrow J/\psi \pi^+ \pi^-$, $\psi(2S) \rightarrow e^+ e^-$ and $J/\psi \rightarrow e^+ e^-$ decays [47].

The $\psi(2S)p$ and $\psi(2S)\pi^-$ mass spectra are investigated and no evidence for contributions from exotic states is found. With a larger data sample a detailed amplitude analysis of this decay could be performed, making it possible to search for small contributions from exotic states.

Acknowledgements

We express our gratitude to our colleagues in the CERN accelerator departments for the excellent performance of the LHC. We thank the technical and administrative staff at the LHCb institutes. We acknowledge support from CERN and from the national agencies: CAPES, CNPq, FAPERJ and FINEP (Brazil); MOST and NSFC (China); CNRS/IN2P3 (France); BMBF, DFG and MPG (Germany); INFN (Italy); NWO (Netherlands); MNiSW and NCN (Poland); MEN/IFA (Romania); MinES and FASO (Russia); MinECo (Spain); SNSF and SER (Switzerland); NASU (Ukraine); STFC (United Kingdom); NSF (USA). We acknowledge the computing resources that are provided by CERN, IN2P3 (France), KIT and DESY (Germany), INFN (Italy), SURF (Netherlands), PIC (Spain), GridPP (United Kingdom), RRCKI and Yandex LLC (Russia), CSCS (Switzerland), IFIN-HH (Romania), CBPF (Brazil), PL-GRID (Poland) and OSC (USA). We are indebted to the communities behind the multiple open-source software packages on which we depend. Individual groups or members have received support from AvH Foundation (Germany), EPLANET, Marie Skłodowska-Curie Actions and ERC (European Union), ANR, Labex P2IO and OCEVU, and Région Auvergne-Rhône-Alpes (France), Key Research Program of Frontier Sciences of CAS, CAS PIFI, and the Thousand Talents Program (China), RFBR, RSF and Yandex LLC (Russia), GVA, XuntaGal and GENCAT (Spain), Herchel Smith Fund, the Royal Society, the English-Speaking Union and the Leverhulme Trust (United Kingdom).

References

- [1] LHCb collaboration, R. Aaij *et al.*, *Measurement of $\sigma(pp \rightarrow b\bar{b}X)$ at $\sqrt{s} = 7$ TeV in the forward region*, Phys. Lett. **B694** (2010) 209, [arXiv:1009.2731](#).
- [2] LHCb collaboration, R. Aaij *et al.*, *Measurement of J/ψ production in pp collisions at $\sqrt{s} = 7$ TeV*, Eur. Phys. J. **C71** (2011) 1645, [arXiv:1103.0423](#).
- [3] LHCb collaboration, R. Aaij *et al.*, *Production of J/ψ and Υ mesons in pp collisions at $\sqrt{s} = 8$ TeV*, JHEP **06** (2013) 064, [arXiv:1304.6977](#).
- [4] LHCb collaboration, R. Aaij *et al.*, *Measurement of forward J/ψ production cross-sections in pp collisions at $\sqrt{s} = 13$ TeV*, JHEP **10** (2015) 172, Erratum *ibid.* **05** (2017) 063, [arXiv:1509.00771](#).
- [5] LHCb collaboration, R. Aaij *et al.*, *Measurement of the b-quark production cross-section in 7 and 13 TeV pp collisions*, Phys. Rev. Lett. **118** (2017) 052002, Erratum *ibid.* **119** (2017) 169901, [arXiv:1612.05140](#).
- [6] LHCb collaboration, R. Aaij *et al.*, *Measurements of the branching fractions for $B_{(s)} \rightarrow D_{(s)}\pi\pi\pi$ and $\Lambda_b^0 \rightarrow \Lambda_c^+\pi\pi\pi$* , Phys. Rev. **D84** (2011) 092001, Erratum *ibid.* **D85** (2012) 039904, [arXiv:1109.6831](#).
- [7] LHCb collaboration, R. Aaij *et al.*, *Measurements of the $\Lambda_b^0 \rightarrow J/\psi\Lambda$ decay amplitudes and the Λ_b^0 polarisation in pp collisions at $\sqrt{s} = 7$ TeV*, Phys. Lett. **B724** (2013) 27, [arXiv:1302.5578](#).
- [8] LHCb collaboration, R. Aaij *et al.*, *Measurement of the differential branching fraction of the decay $\Lambda_b^0 \rightarrow \Lambda\mu^+\mu^-$* , Phys. Lett. **B725** (2013) 25, [arXiv:1306.2577](#).
- [9] LHCb collaboration, R. Aaij *et al.*, *Study of beauty baryon decays to $D^0\text{ph}^-$ and $\Lambda_c^+\text{h}^-$ final states*, Phys. Rev. **D89** (2014) 032001, [arXiv:1311.4823](#).
- [10] LHCb collaboration, R. Aaij *et al.*, *Searches for Λ_b^0 and Ξ_b^0 decays to $K_s^0 p\pi^-$ and $K_s^0 p K^-$ final states with first observation of the $\Lambda_b^0 \rightarrow K_s^0 p\pi^-$ decay*, JHEP **04** (2014) 087, [arXiv:1402.0770](#).
- [11] LHCb collaboration, R. Aaij *et al.*, *Study of beauty hadron decays into pairs of charm hadrons*, Phys. Rev. Lett. **112** (2014) 202001, [arXiv:1403.3606](#).
- [12] LHCb collaboration, R. Aaij *et al.*, *Study of the kinematic dependences of Λ_b^0 production in pp collisions and a measurement of the $\Lambda_b^0 \rightarrow \Lambda_c^+\pi^-$ branching fraction*, JHEP **08** (2014) 143, [arXiv:1405.6842](#).
- [13] LHCb collaboration, R. Aaij *et al.*, *Observation of the $\Lambda_b^0 \rightarrow J/\psi p\pi^-$ decay*, JHEP **07** (2014) 103, [arXiv:1406.0755](#).
- [14] LHCb collaboration, R. Aaij *et al.*, *Differential branching fraction and angular analysis of $\Lambda_b^0 \rightarrow \Lambda\mu^+\mu^-$ decays*, JHEP **06** (2015) 115, [arXiv:1503.07138](#).

- [15] LHCb collaboration, R. Aaij *et al.*, *Study of the productions of Λ_b^0 and \bar{B}^0 hadrons in pp collisions and first measurement of the $\Lambda_b^0 \rightarrow J/\psi pK^-$ branching fraction*, Chin. Phys. C **40** (2016) 011001, [arXiv:1509.00292](#).
- [16] LHCb collaboration, R. Aaij *et al.*, *Observation of $\Lambda_b^0 \rightarrow \psi(2S)pK^-$ and $\Lambda_b^0 \rightarrow J/\psi\pi^+\pi^-pK^-$ decays and a measurement of the Λ_b^0 baryon mass*, JHEP **05** (2016) 132, [arXiv:1603.06961](#).
- [17] LHCb collaboration, R. Aaij *et al.*, *Observation of the $\Lambda_b^0 \rightarrow \Lambda\phi$ decay*, Phys. Lett. B **759** (2016) 282, [arXiv:1603.02870](#).
- [18] LHCb collaboration, R. Aaij *et al.*, *Observations of $\Lambda_b^0 \rightarrow \Lambda K^+ \pi^-$ and $\Lambda_b^0 \rightarrow \Lambda K^+ K^-$ decays and searches for other Λ_b^0 and Ξ_b^0 decays to $\Lambda h^+ h^-$ final states*, JHEP **05** (2016) 081, [arXiv:1603.00413](#).
- [19] LHCb collaboration, R. Aaij *et al.*, *Observation of the suppressed decay $\Lambda_b^0 \rightarrow p\pi^-\mu^+\mu^-$* , JHEP **04** (2017) 029, [arXiv:1701.08705](#).
- [20] LHCb collaboration, R. Aaij *et al.*, *Observation of the decay $\Lambda_b^0 \rightarrow pK^-\mu^+\mu^-$ and a search for CP violation*, JHEP **06** (2017) 108, [arXiv:1703.00256](#).
- [21] LHCb collaboration, R. Aaij *et al.*, *Study of the $D^0 p$ amplitude in $\Lambda_b^0 \rightarrow D^0 p\pi^-$ decays*, JHEP **05** (2017) 030, [arXiv:1701.07873](#).
- [22] LHCb collaboration, R. Aaij *et al.*, *Observation of the decays $\Lambda_b^0 \rightarrow \chi_{c1}pK^-$ and $\Lambda_b^0 \rightarrow \chi_{c2}pK^-$* , Phys. Rev. Lett. **119** (2017) 062001, [arXiv:1704.07900](#).
- [23] LHCb collaboration, R. Aaij *et al.*, *Measurement of the shape of the $\Lambda_b^0 \rightarrow \Lambda_c^+\mu^-\bar{\nu}_\mu$ differential decay rate*, Phys. Rev. D **96** (2017) 112005, [arXiv:1709.01920](#).
- [24] LHCb collaboration, R. Aaij *et al.*, *Measurement of branching fractions of charmless four-body Λ_b^0 and Ξ_b^0 decays*, JHEP **02** (2018) 098, [arXiv:1711.05490](#).
- [25] LHCb collaboration, R. Aaij *et al.*, *Observation of the decay $\Lambda_b^0 \rightarrow \Lambda_c^+ p\bar{p}\pi^-$* , [arXiv:1804.09617](#), submitted to Phys. Lett. B.
- [26] LHCb collaboration, R. Aaij *et al.*, *Precision measurement of the ratio of the Λ_b^0 to \bar{B}^0 lifetimes*, Phys. Lett. B **734** (2014) 122, [arXiv:1402.6242](#).
- [27] LHCb collaboration, R. Aaij *et al.*, *Observation of $J/\psi p$ resonances consistent with pentaquark states in $\Lambda_b^0 \rightarrow J/\psi pK^-$ decays*, Phys. Rev. Lett. **115** (2015) 072001, [arXiv:1507.03414](#).
- [28] LHCb collaboration, R. Aaij *et al.*, *Model-independent evidence for $J/\psi p$ contributions to $\Lambda_b^0 \rightarrow J/\psi pK^-$ decays*, Phys. Rev. Lett. **117** (2016) 082002, [arXiv:1604.05708](#).
- [29] LHCb collaboration, R. Aaij *et al.*, *Evidence for exotic hadron contributions to $\Lambda_b^0 \rightarrow J/\psi p\pi^-$ decays*, Phys. Rev. Lett. **117** (2016) 082003, [arXiv:1606.06999](#).
- [30] ATLAS collaboration, G. Aad *et al.*, *Measurement of the branching ratio $\Gamma(\Lambda_b^0 \rightarrow \psi(2S)\Lambda^0)/\Gamma(\Lambda_b^0 \rightarrow J/\psi\Lambda^0)$ with the ATLAS detector*, Phys. Lett. B **751** (2015) 63, [arXiv:1507.08202](#).

- [31] Belle collaboration, S.-K. Choi *et al.*, *Observation of a resonancelike structure in the $\pi^\pm\psi'$ mass distribution in exclusive $B \rightarrow K\pi^\pm\psi'$ decays*, Phys. Rev. Lett. **100** (2008) 142001, [arXiv:0708.1790](#).
- [32] Belle collaboration, R. Mizuk *et al.*, *Dalitz analysis of $B \rightarrow K\pi^+\psi'$ decays and the $Z(4430)^+$* , Phys. Rev. **D80** (2009) 031104, [arXiv:0905.2869](#).
- [33] Belle collaboration, K. Chilikin *et al.*, *Experimental constraints on the spin and parity of the $Z(4430)^+$* , Phys. Rev. **D88** (2013) 074026, [arXiv:1306.4894](#).
- [34] LHCb collaboration, R. Aaij *et al.*, *Observation of the resonant character of the $Z(4430)^-$ state*, Phys. Rev. Lett. **112** (2014) 222002, [arXiv:1404.1903](#).
- [35] LHCb collaboration, R. Aaij *et al.*, *Model-independent confirmation of the $Z(4430)^-$ state*, Phys. Rev. **D92** (2015) 112009, [arXiv:1510.01951](#).
- [36] BaBar collaboration, B. Aubert *et al.*, *Evidence for $X(3872) \rightarrow \Psi(2S)\gamma$ in $B^\pm \rightarrow X(3872)K^\pm$ decays and a study of $B \rightarrow c\bar{c}\gamma K$* , Phys. Rev. Lett. **102** (2009) 132001, [arXiv:0809.0042](#).
- [37] LHCb collaboration, R. Aaij *et al.*, *Evidence for the decay $X(3872) \rightarrow \Psi(2S)\gamma$* , Nucl. Phys. **B886** (2014) 665, [arXiv:1404.0275](#).
- [38] LHCb collaboration, A. A. Alves Jr. *et al.*, *The LHCb detector at the LHC*, JINST **3** (2008) S08005.
- [39] LHCb collaboration, R. Aaij *et al.*, *LHCb detector performance*, Int. J. Mod. Phys. **A30** (2015) 1530022, [arXiv:1412.6352](#).
- [40] R. Aaij *et al.*, *The LHCb trigger and its performance in 2011*, JINST **8** (2013) P04022, [arXiv:1211.3055](#).
- [41] T. Sjöstrand, S. Mrenna, and P. Skands, *A brief introduction to PYTHIA 8.1*, Comput. Phys. Commun. **178** (2008) 852, [arXiv:0710.3820](#).
- [42] I. Belyaev *et al.*, *Handling of the generation of primary events in GAUSS, the LHCb simulation framework*, J. Phys. Conf. Ser. **331** (2011) 032047.
- [43] D. J. Lange, *The EVTGEN particle decay simulation package*, Nucl. Instrum. Meth. **A462** (2001) 152.
- [44] P. Golonka and Z. Was, *PHOTOS Monte Carlo: A precision tool for QED corrections in Z and W decays*, Eur. Phys. J. **C45** (2006) 97, [arXiv:hep-ph/0506026](#).
- [45] Geant4 collaboration, J. Allison *et al.*, *GEANT4 developments and applications*, IEEE Trans. Nucl. Sci. **53** (2006) 270; Geant4 collaboration, S. Agostinelli *et al.*, *GEANT4: A simulation toolkit*, Nucl. Instrum. Meth. **A506** (2003) 250.
- [46] M. Clemencic *et al.*, *The LHCb simulation application, GAUSS: Design, evolution and experience*, J. Phys. Conf. Ser. **331** (2011) 032023.
- [47] Particle Data Group, M. Tanabashi *et al.*, *Review of particle physics*, Phys. Rev. **D98** (2018) 030001.

- [48] W. D. Hulsbergen, *Decay chain fitting with a Kalman filter*, Nucl. Instrum. Meth. **A552** (2005) 566, [arXiv:physics/0503191](https://arxiv.org/abs/physics/0503191).
- [49] T. Skwarnicki, *A study of the radiative cascade transitions between the Υ' and Υ resonances*, PhD thesis, Institute of Nuclear Physics, Krakow, 1986, DESY-F31-86-02.
- [50] LHCb collaboration, R. Aaij *et al.*, *Observation of J/ψ -pair production in pp collisions at $\sqrt{s} = 7$ TeV*, Phys. Lett. **B707** (2012) 52, [arXiv:1109.0963](https://arxiv.org/abs/1109.0963).
- [51] M. Pivk and F. R. Le Diberder, *sPlot: A statistical tool to unfold data distributions*, Nucl. Instrum. Meth. **A555** (2005) 356, [arXiv:physics/0402083](https://arxiv.org/abs/physics/0402083).
- [52] M. Adinolfi *et al.*, *Performance of the LHCb RICH detector at the LHC*, Eur. Phys. J. **C73** (2013) 2431, [arXiv:1211.6759](https://arxiv.org/abs/1211.6759).
- [53] R. Aaij *et al.*, *Selection and processing of calibration samples to measure the particle identification performance of the LHCb experiment in Run 2*, [arXiv:1803.00824](https://arxiv.org/abs/1803.00824).
- [54] LHCb collaboration, R. Aaij *et al.*, *Measurement of the track reconstruction efficiency at LHCb*, JINST **10** (2015) P02007, [arXiv:1408.1251](https://arxiv.org/abs/1408.1251).
- [55] LHCb collaboration, R. Aaij *et al.*, *Precision luminosity measurements at LHCb*, JINST **9** (2014) P12005, [arXiv:1410.0149](https://arxiv.org/abs/1410.0149).
- [56] S. Jackman, *Bayesian analysis for the social sciences*, John Wiley & Sons, Inc., Hoboken, New Jersey, USA, 2009.
- [57] D. Martínez Santos and F. Dupertuis, *Mass distributions marginalized over per-event errors*, Nucl. Instrum. Meth. **A764** (2014) 150, [arXiv:1312.5000](https://arxiv.org/abs/1312.5000).
- [58] LHCb collaboration, R. Aaij *et al.*, *Measurement of relative branching fractions of B decays to $\Psi(2S)$ and J/ψ mesons*, Eur. Phys. J. **C72** (2012) 2118, [arXiv:1205.0918](https://arxiv.org/abs/1205.0918).
- [59] N. Cabibbo, *Unitary symmetry and leptonic decays*, Phys. Rev. Lett. **10** (1963) 531.

LHCb collaboration

R. Aaij²⁷, B. Adeva⁴¹, M. Adinolfi⁴⁸, C.A. Aidala⁷³, Z. Ajaltouni⁵, S. Akar⁵⁹, P. Albicocco¹⁸, J. Albrecht¹⁰, F. Alessio⁴², M. Alexander⁵³, A. Alfonso Albero⁴⁰, S. Ali²⁷, G. Alkhazov³³, P. Alvarez Cartelle⁵⁵, A.A. Alves Jr⁴¹, S. Amato², S. Amerio²³, Y. Amhis⁷, L. An³, L. Anderlini¹⁷, G. Andreassi⁴³, M. Andreotti^{16,g}, J.E. Andrews⁶⁰, R.B. Appleby⁵⁶, F. Archilli²⁷, P. d'Argent¹², J. Arnau Romeu⁶, A. Artamonov³⁹, M. Artuso⁶¹, K. Arzymatov³⁷, E. Aslanides⁶, M. Atzeni⁴⁴, B. Audurier²², S. Bachmann¹², J.J. Back⁵⁰, S. Baker⁵⁵, V. Balagura^{7,b}, W. Baldini¹⁶, A. Baranov³⁷, R.J. Barlow⁵⁶, S. Barsuk⁷, W. Barter⁵⁶, F. Baryshnikov⁷⁰, V. Batozskaya³¹, B. Batsukh⁶¹, V. Battista⁴³, A. Bay⁴³, J. Beddow⁵³, F. Bedeschi²⁴, I. Bediaga¹, A. Beiter⁶¹, L.J. Bel²⁷, N. Belyi⁶³, V. Bellee⁴³, N. Belloli^{20,i}, K. Belous³⁹, I. Belyaev^{34,42}, E. Ben-Haim⁸, G. Bencivenni¹⁸, S. Benson²⁷, S. Beranek⁹, A. Berezhnoy³⁵, R. Bernet⁴⁴, D. Berninghoff¹², E. Bertholet⁸, A. Bertolin²³, C. Betancourt⁴⁴, F. Betti^{15,42}, M.O. Bettler⁴⁹, M. van Beuzekom²⁷, Ia. Bezshyiko⁴⁴, S. Bhasin⁴⁸, J. Bhom²⁹, S. Bifani⁴⁷, P. Billoir⁸, A. Birnkraut¹⁰, A. Bizzeti^{17,u}, M. Bjørn⁵⁷, M.P. Blago⁴², T. Blake⁵⁰, F. Blanc⁴³, S. Blusk⁶¹, D. Bobulska⁵³, V. Bocci²⁶, O. Boente Garcia⁴¹, T. Boettcher⁵⁸, A. Bondar^{38,w}, N. Bondar³³, S. Borghi^{56,42}, M. Borisyak³⁷, M. Borsato⁴¹, F. Bossu⁷, M. Bouabdil⁹, T.J.V. Bowcock⁵⁴, C. Bozzi^{16,42}, S. Braun¹², M. Brodski⁴², J. Brodzicka²⁹, A. Brossa Gonzalo⁵⁰, D. Brundu²², E. Buchanan⁴⁸, A. Buonaura⁴⁴, C. Burr⁵⁶, A. Bursche²², J. Buytaert⁴², W. Byczynski⁴², S. Cadeddu²², H. Cai⁶⁴, R. Calabrese^{16,g}, R. Calladine⁴⁷, M. Calvi^{20,i}, M. Calvo Gomez^{40,m}, A. Camboni^{40,m}, P. Campana¹⁸, D.H. Campora Perez⁴², L. Capriotti⁵⁶, A. Carbone^{15,e}, G. Carboni²⁵, R. Cardinale^{19,h}, A. Cardini²², P. Carniti^{20,i}, L. Carson⁵², K. Carvalho Akiba², G. Casse⁵⁴, L. Cassina²⁰, M. Cattaneo⁴², G. Cavallero^{19,h}, R. Cenci^{24,p}, D. Chamont⁷, M.G. Chapman⁴⁸, M. Charles⁸, Ph. Charpentier⁴², G. Chatzikonstantinidis⁴⁷, M. Chefdeville⁴, V. Chekalina³⁷, C. Chen³, S. Chen²², S.-G. Chitic⁴², V. Chobanova⁴¹, M. Chrzaszcz⁴², A. Chubykin³³, P. Ciambrone¹⁸, X. Cid Vidal⁴¹, G. Ciezarek⁴², P.E.L. Clarke⁵², M. Clemencic⁴², H.V. Cliff⁴⁹, J. Closier⁴², V. Coco⁴², J.A.B. Coelho⁷, J. Cogan⁶, E. Cogneras⁵, L. Cojocariu³², P. Collins⁴², T. Colombo⁴², A. Comerma-Montells¹², A. Contu²², G. Coombs⁴², S. Coquereau⁴⁰, G. Corti⁴², M. Corvo^{16,g}, C.M. Costa Sobral⁵⁰, B. Couturier⁴², G.A. Cowan⁵², D.C. Craik⁵⁸, A. Crocombe⁵⁰, M. Cruz Torres¹, R. Currie⁵², C. D'Ambrosio⁴², F. Da Cunha Marinho², C.L. Da Silva⁷⁴, E. Dall'Occo²⁷, J. Dalseno⁴⁸, A. Danilina³⁴, A. Davis³, O. De Aguiar Francisco⁴², K. De Bruyn⁴², S. De Capua⁵⁶, M. De Cian⁴³, J.M. De Miranda¹, L. De Paula², M. De Serio^{14,d}, P. De Simone¹⁸, C.T. Dean⁵³, D. Decamp⁴, L. Del Buono⁸, B. Delaney⁴⁹, H.-P. Dembinski¹¹, M. Demmer¹⁰, A. Dendek³⁰, D. Derkach³⁷, O. Deschamps⁵, F. Desse⁷, F. Dettori⁵⁴, B. Dey⁶⁵, A. Di Canto⁴², P. Di Nezza¹⁸, S. Didenko⁷⁰, H. Dijkstra⁴², F. Dordei⁴², M. Dorigo^{42,y}, A. Dosil Suárez⁴¹, L. Douglas⁵³, A. Dovbnya⁴⁵, K. Dreimanis⁵⁴, L. Dufour²⁷, G. Dujany⁸, P. Durante⁴², J.M. Durham⁷⁴, D. Dutta⁵⁶, R. Dzhelyadin³⁹, M. Dziewiecki¹², A. Dziurda²⁹, A. Dzyuba³³, S. Easo⁵¹, U. Egede⁵⁵, V. Egorychev³⁴, S. Eidelman^{38,w}, S. Eisenhardt⁵², U. Eitschberger¹⁰, R. Ekelhof¹⁰, L. Eklund⁵³, S. Ely⁶¹, A. Ene³², S. Escher⁹, S. Esen²⁷, T. Evans⁵⁹, A. Falabella¹⁵, N. Farley⁴⁷, S. Farry⁵⁴, D. Fazzini^{20,42,i}, L. Federici²⁵, P. Fernandez Declara⁴², A. Fernandez Prieto⁴¹, F. Ferrari¹⁵, L. Ferreira Lopes⁴³, F. Ferreira Rodrigues², M. Ferro-Luzzi⁴², S. Filippov³⁶, R.A. Fini¹⁴, M. Fiorini^{16,g}, M. Firlej³⁰, C. Fitzpatrick⁴³, T. Fiutowski³⁰, F. Fleuret^{7,b}, M. Fontana^{22,42}, F. Fontanelli^{19,h}, R. Forty⁴², V. Franco Lima⁵⁴, M. Frank⁴², C. Frei⁴², J. Fu^{21,q}, W. Funk⁴², C. Färber⁴², M. Féo Pereira Rivello Carvalho²⁷, E. Gabriel⁵², A. Gallas Torreira⁴¹, D. Galli^{15,e}, S. Gallorini²³, S. Gambetta⁵², Y. Gan³, M. Gandelman², P. Gandini²¹, Y. Gao³, L.M. Garcia Martin⁷², B. Garcia Plana⁴¹, J. García Pardiñas⁴⁴, J. Garra Tico⁴⁹, L. Garrido⁴⁰, D. Gascon⁴⁰, C. Gaspar⁴², L. Gavard¹⁰, G. Gazzoni⁵, D. Gerick¹², E. Gersabeck⁵⁶, M. Gersabeck⁵⁶, T. Gershon⁵⁰, D. Gerstel⁶, Ph. Ghez⁴, S. Gianì⁴³, V. Gibson⁴⁹, O.G. Girard⁴³, L. Giubega³², K. Gizdov⁵², V.V. Gligorov⁸, D. Golubkov³⁴, A. Golutvin^{55,70}, A. Gomes^{1,a},

I.V. Gorelov³⁵, C. Gotti^{20,i}, E. Govorkova²⁷, J.P. Grabowski¹², R. Graciani Diaz⁴⁰,
 L.A. Granado Cardoso⁴², E. Graugés⁴⁰, E. Graverini⁴⁴, G. Graziani¹⁷, A. Grecu³², R. Greim²⁷,
 P. Griffith²², L. Grillo⁵⁶, L. Gruber⁴², B.R. Gruberg Cazon⁵⁷, O. Grünberg⁶⁷, C. Gu³,
 E. Gushchin³⁶, Yu. Guz^{39,42}, T. Gys⁴², C. Göbel⁶², T. Hadavizadeh⁵⁷, C. Hadjivasiliou⁵,
 G. Haefeli⁴³, C. Haen⁴², S.C. Haines⁴⁹, B. Hamilton⁶⁰, X. Han¹², T.H. Hancock⁵⁷,
 S. Hansmann-Menzemer¹², N. Harnew⁵⁷, S.T. Harnew⁴⁸, T. Harrison⁵⁴, C. Hasse⁴², M. Hatch⁴²,
 J. He⁶³, M. Hecker⁵⁵, K. Heinicke¹⁰, A. Heister¹⁰, K. Hennessy⁵⁴, L. Henry⁷²,
 E. van Herwijnen⁴², M. Heß⁶⁷, A. Hicheur², R. Hidalgo Charman⁵⁶, D. Hill⁵⁷, M. Hilton⁵⁶,
 P.H. Hopchev⁴³, W. Hu⁶⁵, W. Huang⁶³, Z.C. Huard⁵⁹, W. Hulsbergen²⁷, T. Humair⁵⁵,
 M. Hushchyn³⁷, D. Hutchcroft⁵⁴, D. Hynds²⁷, P. Ibis¹⁰, M. Idzik³⁰, P. Ilten⁴⁷, K. Ivshin³³,
 R. Jacobsson⁴², J. Jalocha⁵⁷, E. Jans²⁷, A. Jawahery⁶⁰, F. Jiang³, M. John⁵⁷, D. Johnson⁴²,
 C.R. Jones⁴⁹, C. Joram⁴², B. Jost⁴², N. Jurik⁵⁷, S. Kandybei⁴⁵, M. Karacson⁴², J.M. Kariuki⁴⁸,
 S. Karodia⁵³, N. Kazeev³⁷, M. Kecke¹², F. Keizer⁴⁹, M. Kelsey⁶¹, M. Kenzie⁴⁹, T. Ketel²⁸,
 E. Khairullin³⁷, B. Khanji¹², C. Khurewathanakul⁴³, K.E. Kim⁶¹, T. Kirn⁹, S. Klaver¹⁸,
 K. Klimaszewski³¹, T. Klimkovich¹¹, S. Koliiev⁴⁶, M. Kolpin¹², R. Kopecna¹², P. Koppenburg²⁷,
 I. Kostiuk²⁷, S. Kotriakhova³³, M. Kozeiha⁵, L. Kravchuk³⁶, M. Kreps⁵⁰, F. Kress⁵⁵,
 P. Krokovny^{38,w}, W. Krupa³⁰, W. Krzemien³¹, W. Kucewicz^{29,l}, M. Kucharczyk²⁹,
 V. Kudryavtsev^{38,w}, A.K. Kuonen⁴³, T. Kvaratskheliya^{34,42}, D. Lacarrere⁴², G. Lafferty⁵⁶,
 A. Lai²², D. Lancierini⁴⁴, G. Lanfranchi¹⁸, C. Langenbruch⁹, T. Latham⁵⁰, C. Lazzeroni⁴⁷,
 R. Le Gac⁶, A. Leflat³⁵, J. Lefrançois⁷, R. Lefèvre⁵, F. Lemaitre⁴², O. Leroy⁶, T. Lesiak²⁹,
 B. Leverington¹², P.-R. Li⁶³, T. Li³, Z. Li⁶¹, X. Liang⁶¹, T. Likhomanenko⁶⁹, R. Lindner⁴²,
 F. Lionetto⁴⁴, V. Lisovskyi⁷, X. Liu³, D. Loh⁵⁰, A. Loi²², I. Longstaff⁵³, J.H. Lopes²,
 G.H. Lovell⁴⁹, D. Lucchesi^{23,o}, M. Lucio Martinez⁴¹, A. Lupato²³, E. Luppi^{16,g}, O. Lupton⁴²,
 A. Lusiani²⁴, X. Lyu⁶³, F. Machefert⁷, F. Maciuc³², V. Macko⁴³, P. Mackowiak¹⁰,
 S. Maddrell-Mander⁴⁸, O. Maev^{33,42}, K. Maguire⁵⁶, D. Maisuzenko³³, M.W. Majewski³⁰,
 S. Malde⁵⁷, B. Malecki²⁹, A. Malinin⁶⁹, T. Maltsev^{38,w}, G. Manca^{22,f}, G. Mancinelli⁶,
 D. Marangotto^{21,q}, J. Maratas^{5,v}, J.F. Marchand⁴, U. Marconi¹⁵, C. Marin Benito⁷,
 M. Marinangeli⁴³, P. Marino⁴³, J. Marks¹², P.J. Marshall⁵⁴, G. Martellotti²⁶, M. Martin⁶,
 M. Martinelli⁴², D. Martinez Santos⁴¹, F. Martinez Vidal⁷², A. Massafferri¹, M. Materok⁹,
 R. Matev⁴², A. Mathad⁵⁰, Z. Mathe⁴², V. Matiunin³⁴, C. Matteuzzi²⁰, A. Mauri⁴⁴,
 E. Maurice^{7,b}, B. Maurin⁴³, A. Mazurov⁴⁷, M. McCann^{55,42}, A. McNab⁵⁶, R. McNulty¹³,
 J.V. Mead⁵⁴, B. Meadows⁵⁹, C. Meaux⁶, F. Meier¹⁰, N. Meinert⁶⁷, D. Melnychuk³¹, M. Merk²⁷,
 A. Merli^{21,q}, E. Michelin²³, D.A. Milanes⁶⁶, E. Millard⁵⁰, M.-N. Minard⁴, L. Minzoni^{16,g},
 D.S. Mitzel¹², A. Mogini⁸, J. Molina Rodriguez^{1,z}, T. Mombächer¹⁰, I.A. Monroy⁶⁶, S. Monteil⁵,
 M. Morandin²³, G. Morello¹⁸, M.J. Morello^{24,t}, O. Morgunova⁶⁹, J. Moron³⁰, A.B. Morris⁶,
 R. Mountain⁶¹, F. Muheim⁵², M. Mulder²⁷, C.H. Murphy⁵⁷, D. Murray⁵⁶, A. Mödden¹⁰,
 D. Müller⁴², J. Müller¹⁰, K. Müller⁴⁴, V. Müller¹⁰, P. Naik⁴⁸, T. Nakada⁴³, R. Nandakumar⁵¹,
 A. Nandi⁵⁷, T. Nanut⁴³, I. Nasteva², M. Needham⁵², N. Neri²¹, S. Neubert¹², N. Neufeld⁴²,
 M. Neuner¹², T.D. Nguyen⁴³, C. Nguyen-Mau^{43,n}, S. Nieswand⁹, R. Niet¹⁰, N. Nikitin³⁵,
 A. Nogay⁶⁹, N.S. Nolte⁴², D.P. O'Hanlon¹⁵, A. Oblakowska-Mucha³⁰, V. Obraztsov³⁹,
 S. Ogilvy¹⁸, R. Oldeman^{22,f}, C.J.G. Onderwater⁶⁸, A. Ossowska²⁹, J.M. Otalora Goicochea²,
 P. Owen⁴⁴, A. Oyanguren⁷², P.R. Pais⁴³, T. Pajero^{24,t}, A. Palano¹⁴, M. Palutan^{18,42},
 G. Panshin⁷¹, A. Papanestis⁵¹, M. Pappagallo⁵², L.L. Pappalardo^{16,g}, W. Parker⁶⁰, C. Parkes⁵⁶,
 G. Passaleva^{17,42}, A. Pastore¹⁴, M. Patel⁵⁵, C. Patrignani^{15,e}, A. Pearce⁴², A. Pellegrino²⁷,
 G. Penso²⁶, M. Pepe Altarelli⁴², S. Perazzini⁴², D. Pereima³⁴, P. Perret⁵, L. Pescatore⁴³,
 K. Petridis⁴⁸, A. Petrolini^{19,h}, A. Petrov⁶⁹, S. Petrucci⁵², M. Petruzzo^{21,q}, B. Pietrzyk⁴,
 G. Pietrzyk⁴³, M. Pikies²⁹, M. Pili⁵⁷, D. Pinci²⁶, J. Pinzino⁴², F. Pisani⁴², A. Piucci¹²,
 V. Placinta³², S. Playfer⁵², J. Plews⁴⁷, M. Plo Casasus⁴¹, F. Polci⁸, M. Poli Lener¹⁸,
 A. Poluektov⁵⁰, N. Polukhina^{70,c}, I. Polyakov⁶¹, E. Polycarpo², G.J. Pomery⁴⁸, S. Ponce⁴²,
 A. Popov³⁹, D. Popov^{47,11}, S. Poslavskii³⁹, C. Potterat², E. Price⁴⁸, J. Prisciandaro⁴¹,

C. Prouve⁴⁸, V. Pugatch⁴⁶, A. Puig Navarro⁴⁴, H. Pullen⁵⁷, G. Punzi^{24,p}, W. Qian⁶³, J. Qin⁶³, R. Quagliani⁸, B. Quintana⁵, B. Rachwal³⁰, J.H. Rademacker⁴⁸, M. Rama²⁴, M. Ramos Pernas⁴¹, M.S. Rangel², F. Ratnikov^{37,x}, G. Raven²⁸, M. Ravonel Salzgeber⁴², M. Reboud⁴, F. Redi⁴³, S. Reichert¹⁰, A.C. dos Reis¹, F. Reiss⁸, C. Remon Alepuz⁷², Z. Ren³, V. Renaudin⁷, S. Ricciardi⁵¹, S. Richards⁴⁸, K. Rinnert⁵⁴, P. Robbe⁷, A. Robert⁸, A.B. Rodrigues⁴³, E. Rodrigues⁵⁹, J.A. Rodriguez Lopez⁶⁶, M. Roehrken⁴², A. Rogozhnikov³⁷, S. Roiser⁴², A. Rollings⁵⁷, V. Romanovskiy³⁹, A. Romero Vidal⁴¹, M. Rotondo¹⁸, M.S. Rudolph⁶¹, T. Ruf⁴², J. Ruiz Vidal⁷², J.J. Saborido Silva⁴¹, N. Sagidova³³, B. Saitta^{22,f}, V. Salustino Guimaraes⁶², C. Sanchez Gras²⁷, C. Sanchez Mayordomo⁷², B. Sanmartin Sedes⁴¹, R. Santacesaria²⁶, C. Santamarina Rios⁴¹, M. Santimaria¹⁸, E. Santovetti^{25,j}, G. Sarpis⁵⁶, A. Sarti^{18,k}, C. Satriano^{26,s}, A. Satta²⁵, M. Saur⁶³, D. Savrina^{34,35}, S. Schael⁹, M. Schellenberg¹⁰, M. Schiller⁵³, H. Schindler⁴², M. Schmelling¹¹, T. Schmelzer¹⁰, B. Schmidt⁴², O. Schneider⁴³, A. Schopper⁴², H.F. Schreiner⁵⁹, M. Schubiger⁴³, M.H. Schune⁷, R. Schwemmer⁴², B. Sciascia¹⁸, A. Sciubba^{26,k}, A. Semennikov³⁴, E.S. Sepulveda⁸, A. Sergi^{47,42}, N. Serra⁴⁴, J. Serrano⁶, L. Sestini²³, A. Seuthe¹⁰, P. Seyfert⁴², M. Shapkin³⁹, Y. Shcheglov^{33,†}, T. Shears⁵⁴, L. Shekhtman^{38,w}, V. Shevchenko⁶⁹, E. Shmanin⁷⁰, B.G. Siddi¹⁶, R. Silva Coutinho⁴⁴, L. Silva de Oliveira², G. Simi^{23,o}, S. Simone^{14,d}, N. Skidmore¹², T. Skwarnicki⁶¹, J.G. Smeaton⁴⁹, E. Smith⁹, I.T. Smith⁵², M. Smith⁵⁵, M. Soares¹⁵, I. Soares Lavra¹, M.D. Sokoloff⁵⁹, F.J.P. Soler⁵³, B. Souza De Paula², B. Spaan¹⁰, P. Spradlin⁵³, F. Stagni⁴², M. Stahl¹², S. Stahl⁴², P. Steffko⁴³, S. Stefkova⁵⁵, O. Steinkamp⁴⁴, S. Stemmle¹², O. Stenyakin³⁹, M. Stepanova³³, H. Stevens¹⁰, S. Stone⁶¹, B. Storaci⁴⁴, S. Stracka^{24,p}, M.E. Stramaglia⁴³, M. Straticiuc³², U. Straumann⁴⁴, S. Strokov⁷¹, J. Sun³, L. Sun⁶⁴, K. Swientek³⁰, V. Syropoulos²⁸, T. Szumlak³⁰, M. Szymanski⁶³, S. T'Jampens⁴, Z. Tang³, A. Tayduganov⁶, T. Tekampe¹⁰, G. Tellarini¹⁶, F. Teubert⁴², E. Thomas⁴², J. van Tilburg²⁷, M.J. Tilley⁵⁵, V. Tisserand⁵, M. Tobin³⁰, S. Tolk⁴², L. Tomassetti^{16,g}, D. Tonelli²⁴, D.Y. Tou⁸, R. Tourinho Jadallah Aoude¹, E. Tournefier⁴, M. Trail⁵³, M.T. Tran⁴³, A. Trisovic⁴⁹, A. Tsaregorodtsev⁶, G. Tuci²⁴, A. Tully⁴⁹, N. Tuning^{27,42}, A. Ukleja³¹, A. Usachov⁷, A. Ustyuzhanin³⁷, U. Uwer¹², A. Vagner⁷¹, V. Vagnoni¹⁵, A. Valassi⁴², S. Valat⁴², G. Valenti¹⁵, R. Vazquez Gomez⁴², P. Vazquez Regueiro⁴¹, S. Vecchi¹⁶, M. van Veghel²⁷, J.J. Velthuis⁴⁸, M. Veltri^{17,r}, G. Veneziano⁵⁷, A. Venkateswaran⁶¹, T.A. Verlage⁹, M. Vernet⁵, M. Veronesi²⁷, N.V. Veronika¹³, M. Vesterinen⁵⁷, J.V. Viana Barbosa⁴², D. Vieira⁶³, M. Vieites Diaz⁴¹, H. Viemann⁶⁷, X. Vilasis-Cardona^{40,m}, A. Vitkovskiy²⁷, M. Vitti⁴⁹, V. Volkov³⁵, A. Vollhardt⁴⁴, B. Voneki⁴², A. Vorobyev³³, V. Vorobyev^{38,w}, J.A. de Vries²⁷, C. Vázquez Sierra²⁷, R. Waldi⁶⁷, J. Walsh²⁴, J. Wang⁶¹, M. Wang³, Y. Wang⁶⁵, Z. Wang⁴⁴, D.R. Ward⁴⁹, H.M. Wark⁵⁴, N.K. Watson⁴⁷, D. Websdale⁵⁵, A. Weiden⁴⁴, C. Weisser⁵⁸, M. Whitehead⁹, J. Wicht⁵⁰, G. Wilkinson⁵⁷, M. Wilkinson⁶¹, I. Williams⁴⁹, M.R.J. Williams⁵⁶, M. Williams⁵⁸, T. Williams⁴⁷, F.F. Wilson^{51,42}, J. Wimberley⁶⁰, M. Winn⁷, J. Wishahi¹⁰, W. Wislicki³¹, M. Witek²⁹, G. Wormser⁷, S.A. Wotton⁴⁹, K. Wyllie⁴², D. Xiao⁶⁵, Y. Xie⁶⁵, A. Xu³, M. Xu⁶⁵, Q. Xu⁶³, Z. Xu³, Z. Xu⁴, Z. Yang³, Z. Yang⁶⁰, Y. Yao⁶¹, L.E. Yeomans⁵⁴, H. Yin⁶⁵, J. Yu^{65,ab}, X. Yuan⁶¹, O. Yushchenko³⁹, K.A. Zarebski⁴⁷, M. Zavertyaev^{11,c}, D. Zhang⁶⁵, L. Zhang³, W.C. Zhang^{3,aa}, Y. Zhang⁷, A. Zhelezov¹², Y. Zheng⁶³, X. Zhu³, V. Zhukov^{9,35}, J.B. Zonneveld⁵², S. Zucchelli¹⁵.

¹Centro Brasileiro de Pesquisas Físicas (CBPF), Rio de Janeiro, Brazil

²Universidade Federal do Rio de Janeiro (UFRJ), Rio de Janeiro, Brazil

³Center for High Energy Physics, Tsinghua University, Beijing, China

⁴Univ. Grenoble Alpes, Univ. Savoie Mont Blanc, CNRS, IN2P3-LAPP, Annecy, France

⁵Clermont Université, Université Blaise Pascal, CNRS/IN2P3, LPC, Clermont-Ferrand, France

⁶Aix Marseille Univ, CNRS/IN2P3, CPPM, Marseille, France

⁷LAL, Univ. Paris-Sud, CNRS/IN2P3, Université Paris-Saclay, Orsay, France

⁸LPNHE, Sorbonne Université, Paris Diderot Sorbonne Paris Cité, CNRS/IN2P3, Paris, France

- ⁹*I. Physikalisches Institut, RWTH Aachen University, Aachen, Germany*
- ¹⁰*Fakultät Physik, Technische Universität Dortmund, Dortmund, Germany*
- ¹¹*Max-Planck-Institut für Kernphysik (MPIK), Heidelberg, Germany*
- ¹²*Physikalisches Institut, Ruprecht-Karls-Universität Heidelberg, Heidelberg, Germany*
- ¹³*School of Physics, University College Dublin, Dublin, Ireland*
- ¹⁴*INFN Sezione di Bari, Bari, Italy*
- ¹⁵*INFN Sezione di Bologna, Bologna, Italy*
- ¹⁶*INFN Sezione di Ferrara, Ferrara, Italy*
- ¹⁷*INFN Sezione di Firenze, Firenze, Italy*
- ¹⁸*INFN Laboratori Nazionali di Frascati, Frascati, Italy*
- ¹⁹*INFN Sezione di Genova, Genova, Italy*
- ²⁰*INFN Sezione di Milano-Bicocca, Milano, Italy*
- ²¹*INFN Sezione di Milano, Milano, Italy*
- ²²*INFN Sezione di Cagliari, Monserrato, Italy*
- ²³*INFN Sezione di Padova, Padova, Italy*
- ²⁴*INFN Sezione di Pisa, Pisa, Italy*
- ²⁵*INFN Sezione di Roma Tor Vergata, Roma, Italy*
- ²⁶*INFN Sezione di Roma La Sapienza, Roma, Italy*
- ²⁷*Nikhef National Institute for Subatomic Physics, Amsterdam, Netherlands*
- ²⁸*Nikhef National Institute for Subatomic Physics and VU University Amsterdam, Amsterdam, Netherlands*
- ²⁹*Henryk Niewodniczanski Institute of Nuclear Physics Polish Academy of Sciences, Kraków, Poland*
- ³⁰*AGH - University of Science and Technology, Faculty of Physics and Applied Computer Science, Kraków, Poland*
- ³¹*National Center for Nuclear Research (NCBJ), Warsaw, Poland*
- ³²*Horia Hulubei National Institute of Physics and Nuclear Engineering, Bucharest-Magurele, Romania*
- ³³*Petersburg Nuclear Physics Institute (PNPI), Gatchina, Russia*
- ³⁴*Institute of Theoretical and Experimental Physics (ITEP), Moscow, Russia*
- ³⁵*Institute of Nuclear Physics, Moscow State University (SINP MSU), Moscow, Russia*
- ³⁶*Institute for Nuclear Research of the Russian Academy of Sciences (INR RAS), Moscow, Russia*
- ³⁷*Yandex School of Data Analysis, Moscow, Russia*
- ³⁸*Budker Institute of Nuclear Physics (SB RAS), Novosibirsk, Russia*
- ³⁹*Institute for High Energy Physics (IHEP), Protvino, Russia*
- ⁴⁰*ICCUB, Universitat de Barcelona, Barcelona, Spain*
- ⁴¹*Instituto Galego de Física de Altas Enerxías (IGFAE), Universidade de Santiago de Compostela, Santiago de Compostela, Spain*
- ⁴²*European Organization for Nuclear Research (CERN), Geneva, Switzerland*
- ⁴³*Institute of Physics, Ecole Polytechnique Fédérale de Lausanne (EPFL), Lausanne, Switzerland*
- ⁴⁴*Physik-Institut, Universität Zürich, Zürich, Switzerland*
- ⁴⁵*NSC Kharkiv Institute of Physics and Technology (NSC KIPT), Kharkiv, Ukraine*
- ⁴⁶*Institute for Nuclear Research of the National Academy of Sciences (KINR), Kyiv, Ukraine*
- ⁴⁷*University of Birmingham, Birmingham, United Kingdom*
- ⁴⁸*H.H. Wills Physics Laboratory, University of Bristol, Bristol, United Kingdom*
- ⁴⁹*Cavendish Laboratory, University of Cambridge, Cambridge, United Kingdom*
- ⁵⁰*Department of Physics, University of Warwick, Coventry, United Kingdom*
- ⁵¹*STFC Rutherford Appleton Laboratory, Didcot, United Kingdom*
- ⁵²*School of Physics and Astronomy, University of Edinburgh, Edinburgh, United Kingdom*
- ⁵³*School of Physics and Astronomy, University of Glasgow, Glasgow, United Kingdom*
- ⁵⁴*Oliver Lodge Laboratory, University of Liverpool, Liverpool, United Kingdom*
- ⁵⁵*Imperial College London, London, United Kingdom*
- ⁵⁶*School of Physics and Astronomy, University of Manchester, Manchester, United Kingdom*
- ⁵⁷*Department of Physics, University of Oxford, Oxford, United Kingdom*
- ⁵⁸*Massachusetts Institute of Technology, Cambridge, MA, United States*
- ⁵⁹*University of Cincinnati, Cincinnati, OH, United States*
- ⁶⁰*University of Maryland, College Park, MD, United States*
- ⁶¹*Syracuse University, Syracuse, NY, United States*

- ⁶²*Pontifícia Universidade Católica do Rio de Janeiro (PUC-Rio), Rio de Janeiro, Brazil, associated to* ²
- ⁶³*University of Chinese Academy of Sciences, Beijing, China, associated to* ³
- ⁶⁴*School of Physics and Technology, Wuhan University, Wuhan, China, associated to* ³
- ⁶⁵*Institute of Particle Physics, Central China Normal University, Wuhan, Hubei, China, associated to* ³
- ⁶⁶*Departamento de Física, Universidad Nacional de Colombia, Bogota, Colombia, associated to* ⁸
- ⁶⁷*Institut für Physik, Universität Rostock, Rostock, Germany, associated to* ¹²
- ⁶⁸*Van Swinderen Institute, University of Groningen, Groningen, Netherlands, associated to* ²⁷
- ⁶⁹*National Research Centre Kurchatov Institute, Moscow, Russia, associated to* ³⁴
- ⁷⁰*National University of Science and Technology "MISIS", Moscow, Russia, associated to* ³⁴
- ⁷¹*National Research Tomsk Polytechnic University, Tomsk, Russia, associated to* ³⁴
- ⁷²*Instituto de Física Corpuscular, Centro Mixto Universidad de Valencia - CSIC, Valencia, Spain, associated to* ⁴⁰
- ⁷³*University of Michigan, Ann Arbor, United States, associated to* ⁶¹
- ⁷⁴*Los Alamos National Laboratory (LANL), Los Alamos, United States, associated to* ⁶¹

^a*Universidade Federal do Triângulo Mineiro (UFTM), Uberaba-MG, Brazil*

^b*Laboratoire Leprince-Ringuet, Palaiseau, France*

^c*P.N. Lebedev Physical Institute, Russian Academy of Science (LPI RAS), Moscow, Russia*

^d*Università di Bari, Bari, Italy*

^e*Università di Bologna, Bologna, Italy*

^f*Università di Cagliari, Cagliari, Italy*

^g*Università di Ferrara, Ferrara, Italy*

^h*Università di Genova, Genova, Italy*

ⁱ*Università di Milano Bicocca, Milano, Italy*

^j*Università di Roma Tor Vergata, Roma, Italy*

^k*Università di Roma La Sapienza, Roma, Italy*

^l*AGH - University of Science and Technology, Faculty of Computer Science, Electronics and Telecommunications, Kraków, Poland*

^m*LIFAELS, La Salle, Universitat Ramon Llull, Barcelona, Spain*

ⁿ*Hanoi University of Science, Hanoi, Vietnam*

^o*Università di Padova, Padova, Italy*

^p*Università di Pisa, Pisa, Italy*

^q*Università degli Studi di Milano, Milano, Italy*

^r*Università di Urbino, Urbino, Italy*

^s*Università della Basilicata, Potenza, Italy*

^t*Scuola Normale Superiore, Pisa, Italy*

^u*Università di Modena e Reggio Emilia, Modena, Italy*

^v*MSU - Iligan Institute of Technology (MSU-IIT), Iligan, Philippines*

^w*Novosibirsk State University, Novosibirsk, Russia*

^x*National Research University Higher School of Economics, Moscow, Russia*

^y*Sezione INFN di Trieste, Trieste, Italy*

^z*Escuela Agrícola Panamericana, San Antonio de Oriente, Honduras*

^{aa}*School of Physics and Information Technology, Shaanxi Normal University (SNNU), Xi'an, China*

^{ab}*Physics and Micro Electronic College, Hunan University, Changsha City, China*

[†]*Deceased*